Time-dependent changes in NLRP3 and Nrf2 levels in lipopolysaccharide-induced acute lung injury

RANA DHAR[1*], NING LI[1*], LEJUN ZHANG[1*], YAJUN LI[1], MOHAMMAD NASIRUDDIN RANA[1], XINWEI CAO[1], ZHENGQIANG HU[1], XUEFENG WANG[2], XUYANG ZHENG[3], XUANLI XU[4] and HUIFANG TANG[1,5]

[1]Department of Pharmacology, Sir Run Run Shaw Hospital, Zhejiang University School of Medicine, Hangzhou, Zhejiang 310058; [2]Department of Pharmacy, Second Affiliated Hospital, Zhejiang Chinese Medical University, Hangzhou, Zhejiang 310005; [3]Department of Pediatrics, The Affiliated Hangzhou First People's Hospital, Zhejiang University School of Medicine, Hangzhou, Zhejiang 310006; [4]Department of Respiratory Medicine, First Affiliated Hospital, Zhejiang University School of Medicine, Hangzhou, Zhejiang 310003; [5]Clinical Laboratory, Sir Run Run Shaw Hospital, Zhejiang University School of Medicine, and Key Laboratory of Precision Medicine in Diagnosis and Monitoring Research of Zhejiang Province, Hangzhou, Zhejiang 310016, P.R. China

Received June 22, 2022; Accepted September 20, 2022

DOI: 10.3892/ijmm.2022.5198

Abstract. Acute lung injury (ALI) and acute respiratory distress syndrome (ARDS) are severe clinical conditions with a high mortality rate. Nucleotide-binding oligomerization domain (NOD)-like receptor containing pyrin domain 3 (NLRP3) and nuclear factor E2-related factor 2 (Nrf2) have been reported to be associated with ALI. However, the dynamic changes in the levels of these factors in lipopolysaccharide (LPS)-induced lung injury remain unclear. Thus, the present study aimed to determine the LPS-induced activation of immunological cascades, as well as the NLRP3/Nrf2 signaling pathway at different stages of lung injury. For this purpose, mice were divided into six groups as follows: The control, LPS-4 h, LPS-24 h, LPS-48 h, LPS-96 h and LPS-144 h groups. LPS (4 mg/kg) was administered intratracheally to induce lung injury. Flow cytometry was used to determine the changes in macrophages, neutrophils and T-cell subsets in lung tissue, hematoxylin and eosin staining were used to measure the histopathological changes in lung tissues, ELISA was performed to evaluate the levels of cytokines, western blot analysis was used to measure the levels of inflammatory proteins, and reverse transcription-quantitative PCR used to determine the mRNA level of a target gene. Following LPS administration, evident histopathological damage with neutrophil infiltration was observed which peaked at 48 h. The levels of interleukin-1β, keratinocyte-derived chemokine, macrophage inflammatory protein 2 and tumor necrosis factor a were markedly increased in bronchoalveolar lavage fluid and serum from the mice, and these levels peaked at 4 h. Moreover, LPS promoted Toll like receptor-4 expression and reactive oxygen species production, thus activating NLRP3/Nrf2 signaling and pyroptosis. Collectively, the present study demonstrates that LPS triggers multiple inflammatory molecules and immune cells during ALI, which may be closely involved in the irregular redox status, NLRP3/Nrf2 pathway and pyroptosis.

Correspondence to: Dr Xuanli Xu, Department of Respiratory Medicine, First Affiliated Hospital, Zhejiang University School of Medicine, 79 Qingchun Road, Hangzhou, Zhejiang 310003, P.R. China
E-mail: pipilili@zju.edu.cn

Dr Huifang Tang, Department of Pharmacology, Sir Run Run Shaw Hospital, Zhejiang University School of Medicine, 388 Yuhangtang Road, Hangzhou, Zhejiang 310058, P.R. China
E-mail: tanghuifang@zju.edu.cn

*Contributed equally

Key words: lung injury, immune cells, inflammasome, Nrf2, pyroptosis

Introduction

Acute respiratory distress syndrome (ARDS) is categorized as a minor disease, according to the Berlin definition (1). However, ARDS and acute lung injury (ALI) lead to major severe respiratory failure worldwide, and are associated with a high morbidity and mortality due to increased vascular permeability, alveolar-capillary membrane dysfunction, the flooding of protein-rich fluid, alveolar hemorrhage and fibrin deposition (2,3). Following exposure to exogenous irritants, such as lipopolysaccharide (LPS), the excessive accumulations and responses of immune cells, including macrophages and neutrophils in the infected area, are the key factors involved in the pathogenesis of ALI/ARDS (4,5).

LPS is a major component of the outer membrane of Gram-negative bacteria that binds to Toll like receptor-4 (TLR-4), thus leading to the secretion of pro-inflammatory cytokines via various signaling pathways (6,7). Previous studies have demonstrated that LPS may directly affect T-cell activity through the TLR ligand (8,9), alter the ratio of

$CD4^+/CD8^+$ T-cells, and recruit neutrophils and macrophages into the inflamed area (10). Based on their function and location, macrophages present in the lungs are mainly recognized as alveolar macrophages (AMs) and interstitial macrophages (IMs) (11). Importantly, during the process of ALI, AMs exert a host-protective effect by killing microorganisms, secreting large amounts of reactive oxygen radicals and tumor necrosis factor-a (TNF-a) (12); IMs have more efficient functions by releasing immunoregulatory cytokines, such as interleukin (IL)-1β, keratinocyte-derived chemokine (CXCL1/KC) and macrophage inflammatory protein 2 (MIP-2), inducing a specific immune reaction in the pathogenesis of ALI/ARDS (13).

There is also evidence to indicate that activated $CD4^+$ T-cells are involved in ALI and regulate cytotoxic T-lymphocyte antigen 4 (CTLA4) following exposure to LPS (14). In addition to $CD4^+$ T-cells, transcription factors, such as retinoic acid receptor-related orphan nuclear receptor γt (RORγt) trigger the clonal expansion of pro-inflammatory Th17 cells (15). Existing evidence suggests that the activation of the Th17 immune response enhances the inflammatory response in various inflammatory and autoimmune disorders (16). Previous studies have documented that the number of $CD4^+/CD8^+$ cells is markedly increased in the lower respiratory tract area of lung injury (17,18). The role of excessive immune activation and the cytokine storm in lung injury induced by COVID-19 has become a consensus (19,20). However, to date, the interaction between T-cells and lung injury-mediated dysfunction has not yet been fully elucidated. Therefore, further in-depth, systematic and time-dependent studies on T-cell subsets ($CD4^+/CD8^+$ ratio) and cytokine production, as well as the related molecular mechanisms are warranted.

Nuclear factor E2-related factor 2 (Nrf2) and the nucleotide-binding oligomerization domain (NOD)-like receptor containing pyrin domain 3 (NLRP3) inflammasome are both regulated by reactive oxygen species (ROS) under inflammatory conditions (21). Previous studies have demonstrated that Nrf2 plays a positive role in acute and chronic inflammatory diseases (22,23). Under conditions of cellular stress, Nrf2 is released from Kelch-like ECH-associated protein 1 (Keap1) through the proteasomal pathway, and subsequently, Nrf2 translocated to the nucleus to initiate the gene transcription, such as heme oxygenase 1 (HO-1), NAD(P)H dehydrogenase [quinone] 1 (NQO1) and glutathione S-transferase-α. (24). The inflammasome is a multifunctional protein complex composed of inactive NLRP3, adaptor protein apoptosis-associated speck-like protein containing a CARD (ASC) and caspase-1. Subsequently, activated caspase-1 leads to changes in the form of IL-1β and IL-18 from a premature to a mature one. Notably, these are the important indications of pyroptosis (25,26). It has also been observed that Nrf2 is critical for NLRP3 inflammasome activation by ASC oligomerization (27). Previous studies have suggested that Nrf2 deficiency contributes to the alleviation NLRP3 expression in acute and chronic inflammatory diseases, and these results demonstrate an unexpected pro-inflammatory effect of Nrf2 (22,23). In addition, the time-dependent, pro-inflammatory role of Nrf2 remains a contradictory and undefined issue. To date, the immunomodulatory and pro-inflammatory potential of LPS in the NLRP3/Nrf2 pathway has not yet been extensively investigated in a time-dependent manner in an *in vivo* model, at least to the best of our knowledge.

Moreover, caspase-8 is a critical regulator that activates the cleavage of gasdermin D (GSDMD)-dependent cell death (28,29). Cleaved-GSDMD promotes membrane pores, thus leading to the release of cytokine such as IL-1β and others in the inflamed area (30). Therefore, understanding these cell death processes is essential for the development of drugs for the treatment of ALI.

The present study established acute and sub-chronic models of ALI via the intratracheal instillation of 4 mg/kg LPS. Taken together, the present study demonstrated the changes of the potential inflammatory molecules and immune-related pathways in the lung injury model at different time points. Moreover, the inflammatory cell profiles in bronchoalveolar lavage fluid (BALF), and multiple immune cell distribution and the redox status in lung tissue, as well as the activation of the Nrf2/NLRP3 signaling pathway and pyroptosis in the lungs of mice with LPS-induced ALI were also determined.

Materials and methods

Mouse model of intratracheal injection of LPS and experimental design. In the present study, 30 male C57/B6 mice, 6-7 weeks old and weighing 20-25 g, were purchased from SLAC Laboratory Animal (certificate no: SCXK2017-0016). All animal experiments were approved by the Animal Care and Ethics Committee of Zhejiang University, Hangzhou, China. All efforts were made to minimize animal suffering. The mice were kept under standard day/night (12 h light/12 h dark cycle, 45-55% relative humidity and a temperature of 23-25˚C) and pathogen-free conditions. The mice were randomly divided into six groups of 5 mice in each (the control, LPS 4 h, LPS 24 h, LPS 48 h, LPS 96 h and LPS 144 h groups).

First, the mice were anaesthetized with Avertin (2,2,2-tribromoethanol; 0.2 ml/10 g; MilliporeSigma at 240 mg/kg by an intraperitoneal (i.p.) injection according to body weight. After 5 min, the mice were place on the surgical tray in an appropriate position. The neck skin was then sterilized with 75% ethanol, the skin was cut using forceps and scissors, the neck skin was opened, and the tracheal area was isolated very carefully to make the airway visible. Subsequently, LPS (4 mg/kg body weight, *Escherichia coli*, 0111: B4, MilliporeSigma) was injected intratracheally into the mice using a microsyringe. LPS (4 mg/kg) was used as previously described (31,32). In the control group, the same volumes of 0.9% sodium chloride (NaCl) were administrated intratracheally. At the different time points, the mice were deeply anaesthetized and sacrificed for further analysis. Of note, no mice died during the modelling or treatment process in the present study.

Sample collection. The mice were sacrificed at 4, 24, 48, 96 and 144 h after the LPS administration. For euthanasia, the mice (control group and LPS groups) were deeply anesthetized with Avertin (2,2,2-tribromoethanol; 480 mg/kg by i.p. injection. A few minutes later, the heart rate of the mice disappeared due to an anesthesia overdose. Blood was then collected by enucleating the mouse eyeball and this was preserved at 4˚C for 16-18 h. After 16-18 h, the blood

samples were centrifuged at 2,000 x g, 4˚C for 10 min, and the supernatant (upper layer) was collected as serum samples and preserved at -80˚C for determining cytokine levels. Subsequently, a tracheal cannula was used to collect 0.5 ml BALF by injecting ice-cold 1X PBS (Beijing Solarbio Science & Technology Co., Ltd.) into the lungs of mice (twice). The BALF was then centrifuged at 2,000 x g for 10 min at 4˚C. The BALF supernatant and blood serum were then collected and kept at -80˚C for the measurement of cytokine levels. The third part of the right lung was used to perform histopathological examinations; the first lobe of the left lung was used for flow cytometric analysis and the remaining lung lobes were frozen at -80˚C for use in western blot analysis, reverse transcription-quantitative PCR (RT-qPCR) and ROS generation analysis.

Histopathological examination. For histological analysis, the lung tissue was fixed in 10% neutral formalin for 48-72 h at room temperature, embedded in paraffin, and sectioned at a thickness of 4 μm. Following deparaffinization and rehydration using a series of laboratory graded alcohol at different percentages (75%; 85%; 95%-I; 95%-II; 95% alcohol-III, dimethyl benzene-I and dimethyl benzene-II). Alcohol and dimethyl benzene were obtained from Sinopharm Chemical Reagent Co., Ltd. and Haoke Biological Technology Co., Ltd., respectively and the sections were stained with hematoxylin for 5 min and eosin solution for 10-12 sec at room temperature (Nanjing Jiancheng Technology Co. Ltd.), and the tissue sections were rinsed under running water. Finally, lung structures were observed under a full slide scanning microscope (VS200 digital slide scanner BX51, Olympus Corporation). The histopathological findings were then determined based on neutrophil infiltration in the lung tissue. The histopathological status of lung injury was scored according to the Official American Thoracic Society Workshop Report (33). The parameters included the following: a) Neutrophils in the alveolar space; b) neutrophils in the interstitial space; c) hyaline membranes; d) proteinaceous debris filling the airspaces; and e) alveolar septal thickening. The total score was calculated using the following formula: Score=[(20 x a) + (14 x b) + (7 x c) + (7 x d) + (2 x e)]/(number of fields x100).

Determination of cytokine levels in BALF and serum using enzyme-linked immunosorbent assay (ELISA). The collected BALF and blood were centrifuged at 1,000 x g for 8 min at 4˚C, and the supernatant of BALF and serum was used to evaluate the production of inflammatory cytokines using ELISA kits, such as IL-1β (cat. no. DY401), CXCL1/KC (cat. no. DY453), MIP-2 (cat. no. DY452), TNF-α (cat. no. DY410) (all from R&D Systems, Inc.) following the manufacturer's protocol. The optical density was detected at 450 nm using a microplate reader (BioTek Instruments, Inc.). The result sample value was subtracted from the bank value. The levels of IL-1β, CXCL1/KC, MIP-2 and TNF-α were finally expressed in pg/ml.

Flow cytometric analysis. Single-cell suspensions were prepared from the left lung tissues of the mice by cutting these into small sections and digesting these with type I collagenase (3 mg/ml, MilliporeSigma) and DNase I (30 μg/ml) for 45 min at 37˚C in RPMI-1640 medium (cat. no. 10040, Corning, Inc.). The digested lungs were mechanically disrupted using the flat portion of a plunger from a 3-ml syringe, then through a sterile filter (100 μm, Falcon, BD Biosciences) followed by an additional 40-μm strainer (Falcon, BD Biosciences). Red blood cells were lysed with 150 mM NH_4Cl, 10 mM $KHCO_3$ and 0.1 mM EDTA. Following two washes with phosphate-buffered saline (PBS), (Beijing Solarbio Science & Technology Co., Ltd.), the cells were stained with the Zombie Aqua™ Fixable Viability kit (cat. no. 423101; BioLegend, Inc.) in the dark for 15-30 min at room temperature, followed by washing once with cell staining buffer. Following the isolation of live cells, BUV395 rat anti-mouse CD45 (1:80; cat. no. 564279), PerCP-Cy™5.5 hamster anti-mouse CD3e (1:80; cat. no. 551163), FITC rat anti-mouse CD4 (1:80; cat. no. 557307), APC-Cy™7 rat anti-mouse CD8a (1:80; cat. no. 557654), PE-Cy™7 rat anti-mouse Ly-6G (1:80; cat. no. 560601), PE rat anti-mouse F4/80 (1:80; cat. no. 565410), BV650 rat anti-CD11b (1:80; cat. no. 563402) antibodies were used with incubation at 4˚C for 30 min. All antibodies were purchased from BD Biosciences. Samples were evaluated using a CytoFLEX LX flow cytometry analyzer (Beckman Coulter, Inc.). The results were analyzed using CytExpert Version 2.4 software (Beckman Coulter, Inc.).

Total RNA isolation and RT-qPCR. RNA was isolated from lung tissues using RNAiso plus (Takara Bio, Inc.) according to the manufacturer's instructions and reverse transcribed into cDNA using the PrimeScript™ RT reagent kit from Takara Bio, Inc. qPCR was performed on the Bio-Rad C1000 real-time PCR system using SYBR-Green Master Mix reagent (Bio-Rad Laboratories, Inc.). The PCR amplification reaction was as follows: 95˚C for 30 sec, and subjected to 40 cycles of 95˚C for 3 sec and 62˚C for 30 sec. Primers were designed using the primer bank website (https://pga.mgh.harvard.edu/primerbank/). The data were evaluated using the $2^{-\Delta\Delta Cq}$ formula for relative quantitation and normalized to glyceraldehyde-3-phosphate dehydrogenase (GAPDH) (34). The sequences of the primers for mouse gene expression are listed in Table I (forward and reverse).

Western blot analysis. Total protein was extracted from the lung tissue using cold radio immunoprecipitation assay (RIPA) lysis buffer (including 1% protease inhibitor cocktail (Roche Diagnostics), 2% PMSF (MilliporeSigma) and 1X PhosSTOP (Roche Diagnostics) and centrifuged at 10,000 x g at 4˚C for 10 min. The protein concentration was evaluated using quick start Bradford 1X dye reagent (Bio-Rad Laboratories, Inc.). Subsequently, 5X loading buffer (Beyotime Institute of Biotechnology, Inc.) was added to the protein sample and then denatured at 100˚C for 5 min. Subsequently, 12% sodium dodecyl sulfate-polyacrylamide gel electrophoresis (SDS-PAGE) was used to separate the proteins. The equivalent loading of the gel was determined by quantitation of the protein and by re-probing the membranes for GAPDH detection. Isolated proteins were electroblotted onto nitrocellulose (NC) membranes (BioTrace NT membranes, Gelman Laboratory) for 70 to 90 min at 300 mA (Mini-protein II System, Bio-Rad Laboratories, Inc.) and blocked for h at room temperature with Tris-buffered saline containing 5% BSA. The membranes were

Table I. Sequences of the primers used in the present study.

Number	Primer name	Forward primer (5'-3')	Reverse primer (5'-3')
I	TLR-4	CGCTTTCACCTCTGCCTTCACTACAG	ACACTACCACAATAACCTTCCGGCTC
II	Nrf2	TCTTGGAGTAAGTCGAGAAGTGT	GTTGAAACTGAGCGAAAAAGGC
III	GAPDH	CATCACTGCCACCCAGAAGACTG	ATGCCAGTGAGCTTCCCGTTCAG

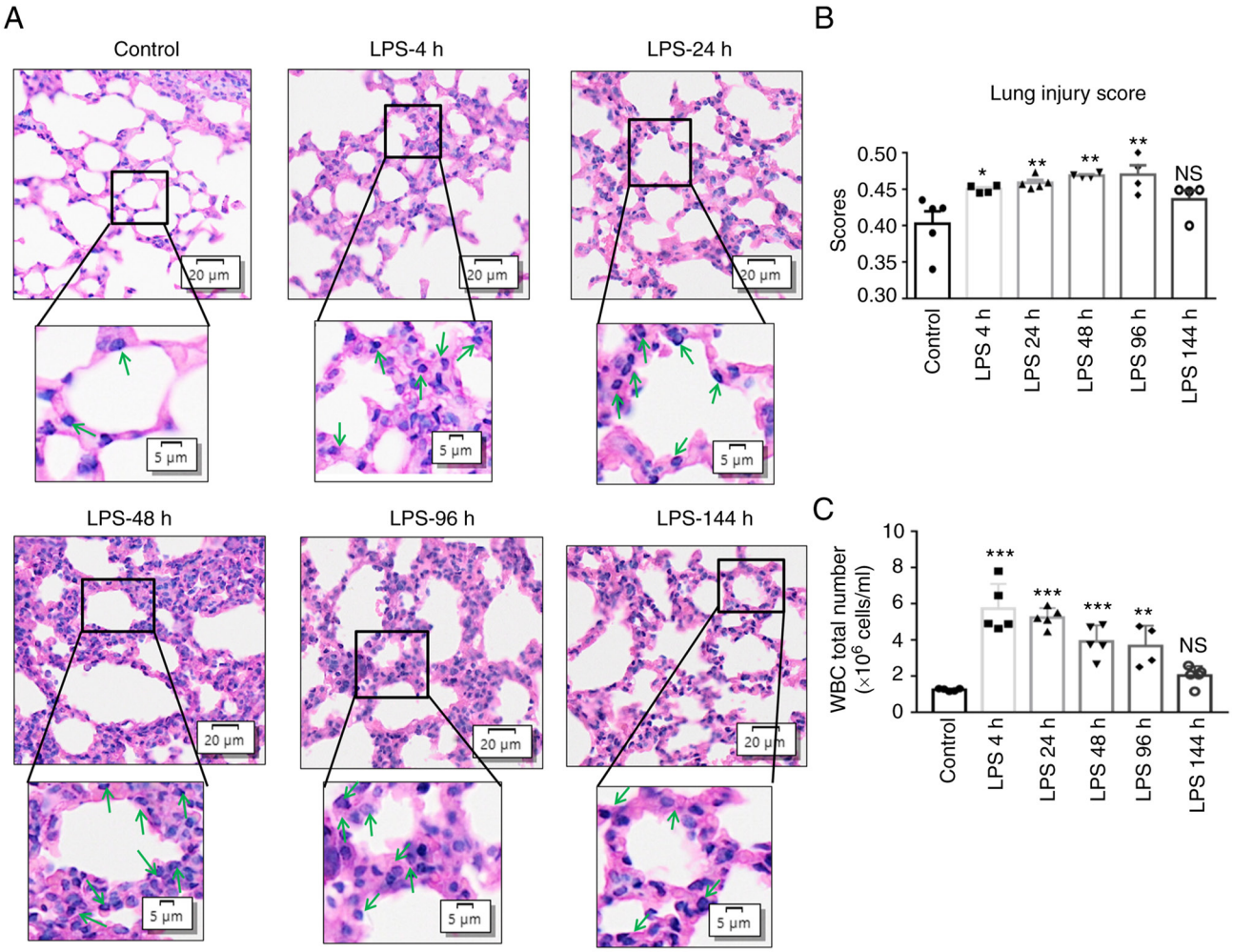

Figure 1. Time-dependent pathological effects in the model of LPS-induced acute lung injury. C57BL/6 mice were exposed to 4 mg/kg LPS via intratracheal installation and 0.9% NaCl was administered to the control mice. Lung tissues and BALF were collected, after 4, 24, 48, 96 and 144 h of LPS exposure and from the control mice. (A) Histological structures of right lung lobes stained with H&E for the LPS groups at different time points and the control group (scale bars: Upper panels, 20 μM; lower panels, 5 μM). Representative results from 5 mice are shown for each group. H&E staining represents the structure of neutrophils (green arrows). (B) Lung injury scores in lung tissue from mice exposed to LPS. (C) Number of WBCs in BALF. Values are presented as the mean ± SEM, n=4-5 mice per group. (C) One-way ANOVA followed by the Bonferroni test and (B) the Kruskal-Wallis test followed by Dunn's post hoc test were used to analyze significant differences between the different time points of the LPS groups vs. the control. *P<0.05, **P<0.01 and ***P<0.001, vs. control. NS, not significant; LPS, lipopolysaccharide; BALF, bronchoalveolar lavage fluid; H&E, hematoxylin and eosin; WBC, white blood cell.

then incubated with the following primary antibodies: TLR-4 (1:1,000; cat. no. ab13867, Abcam), anti-NLRP3 (1:1,000; cat. no. AG-20B-0014, Adipogen Life Sciences); anti-procaspase-1/cleaved caspase-1 (1:1,000; cat. no. ab179515, Abcam), p-Nrf2 (1:1,000; cat. no. db523, Diagbio), (http://www.diagbio.com/), anti-Nrf2 antibody (1:1,000; cat. no. ab137550, Abcam); anti-Keap1 antibody (1:1,000; cat. no. ab119403, Abcam), aAnti-GSDMD antibody (1:1,000; cat. no. ab155233, Abcam), anti-caspase-8 (1:1,000; cat. no. ab227430, Abcam), anti-ASC (1:1,000; cat. no. sc-514559, Santa Cruz Biotechnology, Inc.) and anti-GAPDH (1:5,000; cat. no. db106, Diagbio) at room temperature overnight. After washing with 1X TBST, the membranes were incubated with HRP-conjugated secondary antibodies (1:5,000; IRDye 800CW goat anti-rabbit; IRDye 680CW goat anti-mouse; LI-COR Biosciences) for 1.5 h at room temperature. The membranes were washed three times with 1X TBST, 5 min for each time. Images were captured using an Oddessy CLx infrared laser dual color imaging analysis system (Image Studio Ver 5.2, LI-COR Biosciences). The density of each protein band on the membrane is reported

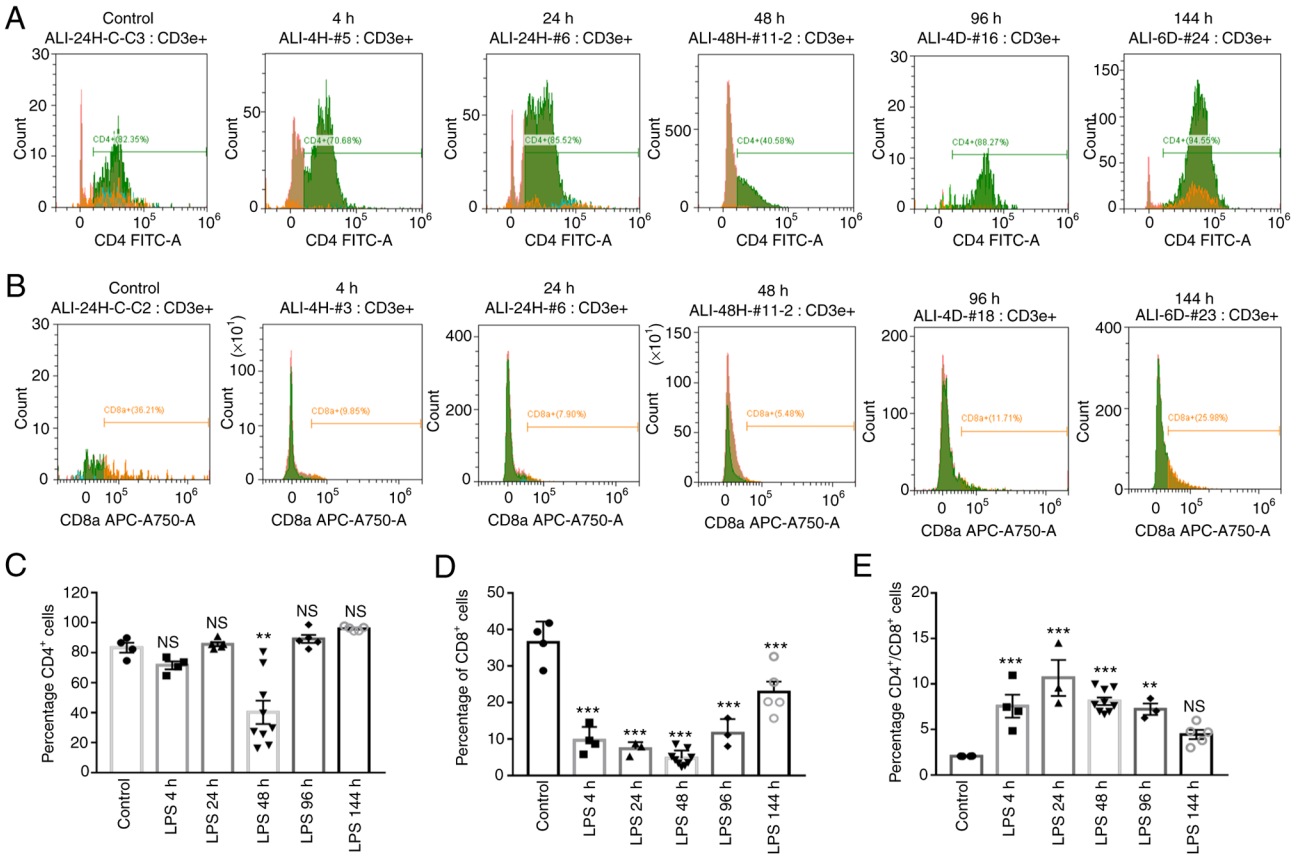

Figure 2. Regulation of $CD4^+$, $CD8^+$ cells and the ratio of $CD4^+$ to $CD8^+$ responses by LPS. C57BL/6 mice were exposed to 4 mg/kg LPS via intratracheal installation for 4, 24, 48, 96 and 144 h, and 0.9% NaCl was administered to the control mice orally. Lung tissues were digested and stained with CD4 FIT C A (marker of $CD4^+$ T-cells) CD8a APC-A750-A (marker of $CD8^+$ T-cells). (A and B) The percentages of $CD4^+$ and $CD8^+$T cells in lung tissue were determined using flow cytometry. (C-E) $CD4^+$, $CD8^+$T-cells, and the $CD4^+/CD8^+$ ratios are presented in bar graphs. The results are expressed as the mean ± SEM (n=4-5 animals in each group). One-way ANOVA followed by the Bonferroni test were used to analyze significant differences among the different time points of the LPS group vs. the control. **P<0.01 and ***P<0.001, vs. control. NS, not significant; LPS, lipopolysaccharide.

as the densitometric ratio between the protein of interest and GAPDH.

Measurement of ROS generation. ROS production in lung tissues was estimated using the method described in the study by Socci *et al* (35), with minor modifications. Homogenates of tissue samples were prepared using ice-cold 40 mM Tris-HCl buffer (pH 7.4). Following sonication, tissue samples were diluted with 0.25% with ice-cold Tris buffer. Subsequently, 100 μl sample solution was used to determine the protein concentration. The remaining 0.25% pf the solution was divided into two equal portions; one portion was mixed with 5 μM dichlorodihydrofluorescein diacetate (DCFH-DA; MilliporeSigma) in methanol, and the other portion was used as a blank (100 μl methanol). All samples were then incubated in a water bath (37˚C) for 45 min. The DCF fluorescence intensities of the samples were detected using a Varioskan Flash micro-plate reader (Thermo Fisher Scientific, Inc.) at excitation and emission wavelengths of 485 and 525 nm, respectively.

Statistical analysis. Statistical analysis was performed using Graph prism 7 software (Graphpad Software, Inc.). The data are presented as the mean ± SEM (n=4-5 mice per group). Differences between groups were determined using one-way analysis of variance (ANOVA) followed by the Bonferroni correction for the comparison of selected column pairs, and the Kruskal-Wallis test followed by Dunn's post hoc test. A value of P<0.05 was considered to indicate a statistically significant difference.

Results

LPS induces lung injury in a time-dependent manner. The most crucial pathological feature of LPS-induced ALI is the accumulation and activation of neutrophils in lung tissues. As shown in Fig. 1A, LPS induced pathological changes in the lung tissues of the mice at 4, 24, 48, 96 and 144 h when compared with the control group, and the highest lung injury scores were recorded from the LPS-4 h to LPS-96 h groups; the scores then exhibited a decreasing trend in the LPS-144 h group (Fig. 1B). Additionally, LPS exposure also resulted in the highest number of white blood cells (WBCs) compared with the control group, with a significant difference up to 96 h of LPS administration, with an increasing trend from 4 h (Fig. 1C). From 4 to 96 h after LPS administration, the features of lung injury were more evident. Notably, no detectable histological damage was observed in the control group.

LPS induces the time-dependent activation of T-cell subsets in lung tissue. T-cell subsets are critical mediators of immune

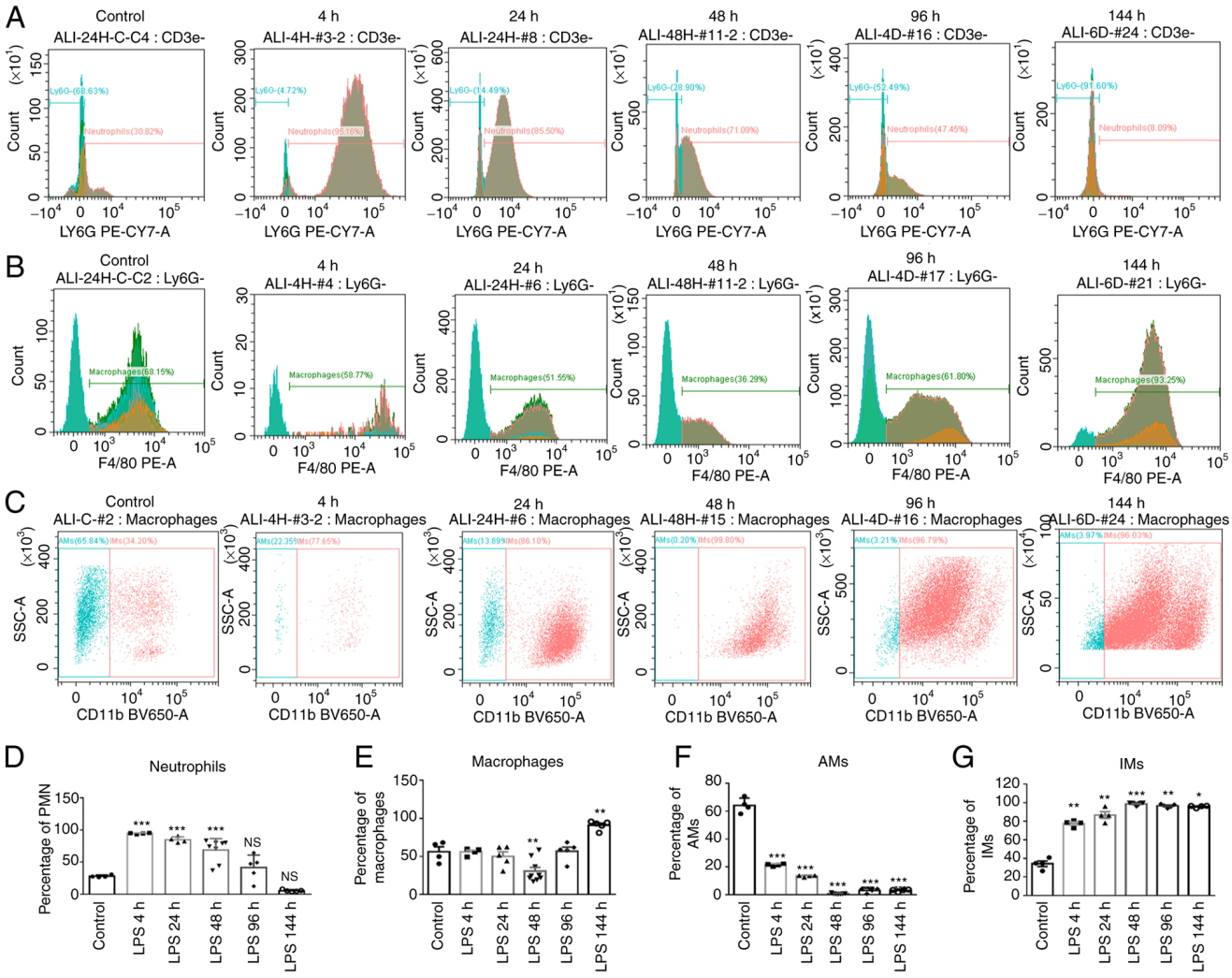

Figure 3. Neutrophils, macrophages, AMs and IMs respond differentially to LPS in the model of ALI. C57BL/6 mice were exposed to 4 mg/kg LPS via intratracheal installation for 4, 24, 48, 96 and 144 h, and 0.9% NaCl was administered to the control mice orally. Lung cells isolated at indicated time points and stained for F4/80 (marker of macrophages), F4/80$^+$CD11b$^-$ (marker of AMs), LY6G PE-CY7A (stained for neutrophils), and F4/80$^+$CD11b$^+$ (marker of IMs). (A-C) Flow cytometric analysis of neutrophils, macrophages, AMs and IMs. (D-G) The percentages of indicated cell populations are presented in bar graphs. The results are representative of five independent mice in each group (mean ± SEM, n=5). One-way ANOVA followed by the Bonferroni test were used to analyze significant differences among the different time points of the LPS group vs. the control. *P<0.05, **P<0.01 and ***P<0.001, vs. control. NS, not significant; LPS, lipopolysaccharide; AMs, alveolar macrophages; IMs, interstitial macrophages.

responses. A previous study demonstrated that the function of T-helper cells was associated with the polarization, recruitment and activation of immune cells during inflammation (36). The present study compared the subpopulation, composition and activation/differentiation of T-cells between the LPS-exposed groups and the control group, in which cells were stained with CD4 FITCA (a marker of CD4$^+$ T-cells) CD8a APC-A750-A (a marker of CD8$^+$ T-cells). As shown in the flow cytometry images (Fig. 2A and B) following exposure to LPS, the numbers of CD4$^+$ T-cells increased to 70.68, 85.52, 40.58, 88.27 and 94.55% in the LPS-4 h, LPS-24 h, LPS-96 h and LPS-144 h groups, respectively, although there were no significant differences relative to the control group (Fig. 2C); of note, in lung tissue from mice exposed to LPS, the numbers of CD8$^+$ T-cells were significantly inhibited at the different time points [LPS-4 h (9.85%); LPS-24 h (7.90%); LPS-48 h (5.48%); LPS-96 h (11.71%) and LPS-144 h (25.98%)] (Fig. 2D). In addition, all LPS-exposed groups had significantly higher CD4$^+$ to CD8$^+$ ratios than the normal control group, and the highest peak of CD4$^+$/CD8$^+$ T-cell ratios was identified in the LPS-24 h group (Fig. 2E). These results thus indicated that the abnormal differentiation of T-cells in responses to LPS was associated with aberrant cytokine production in downstream signaling pathways in ALI.

Time-dependent activation of neutrophil and alveolar/interstitial macrophages in lung tissue. The recruitment of macrophages and neutrophils plays a crucial role in the process of ALI. Following LPS stimulation, the whole left lung lobes from mice were digested and stained; there was a significant increase in the staining for F4/80 (a marker of macrophages) in the LPS-144 h group by 25.1% compared to the control group (Fig. 3B and E). Double immunostaining of the lung tissues confirmed that the F4/80 and CD11b$^+$ macrophages were confined to the interstitial compartment, and the numbers of IMs were significantly increased at 4 to 144 h following exposure to LPS (Fig. 3C and G). Additionally, the intratracheal instillation of LPS induced neutrophil recruitment into the

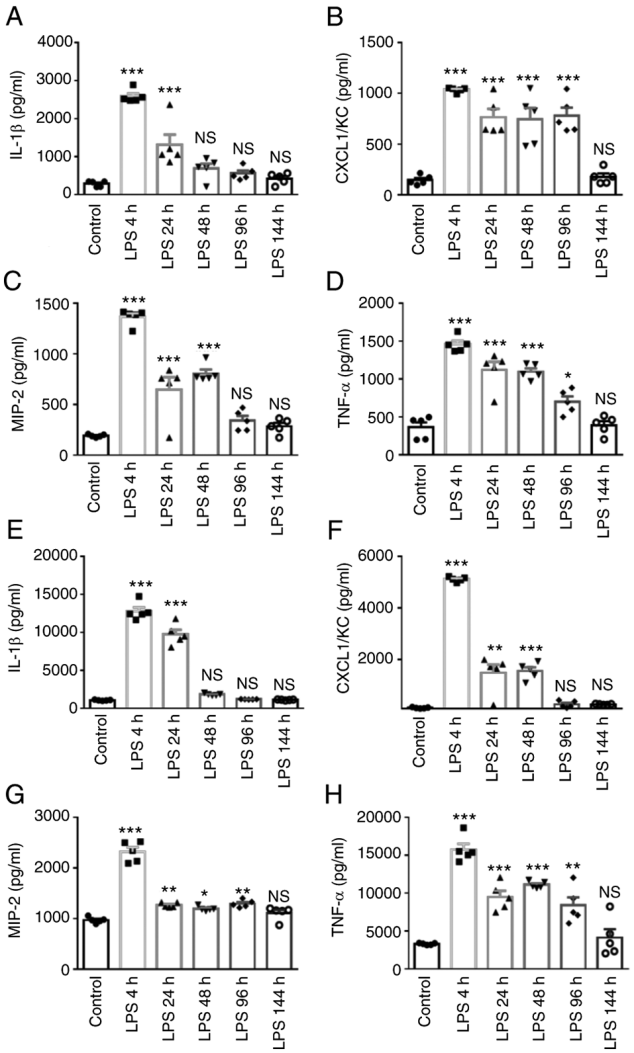

Figure 4. Time-dependent effects on pro-inflammatory cytokines in BALF and serum from mice with LPS-induced lung injury. C57BL/6 mice were exposed to with 4 mg/kg LPS via intratracheal installation for 4, 24, 48, 96 and 144 h, and 0.9% NaCl was administered to the control mice orally. BALF and serum were collected after for 4, 24, 48, 96 and 144 h of LPS exposure and from the control mice. The cytokine levels in (A-D) BALF and (E-H) serum were measured using ELISA and are shown as (A and E) IL-1β, (B and F) CXCL1/KC; (C and G) MIP-2; (D and H) TNF-α accordingly. The results are expressed as the mean ± SEM (n=5 animals in each group). One-way ANOVA followed by the Bonferroni test were used to analyze significant differences among the different time points of the LPS group vs. the control. *P<0.05, **P<0.01 and ***P<0.001, vs. control. NS, not significant; LPS, lipopolysaccharide; BALF, bronchoalveolar lavage fluid; MIP-2, macrophage inflammatory protein 2.

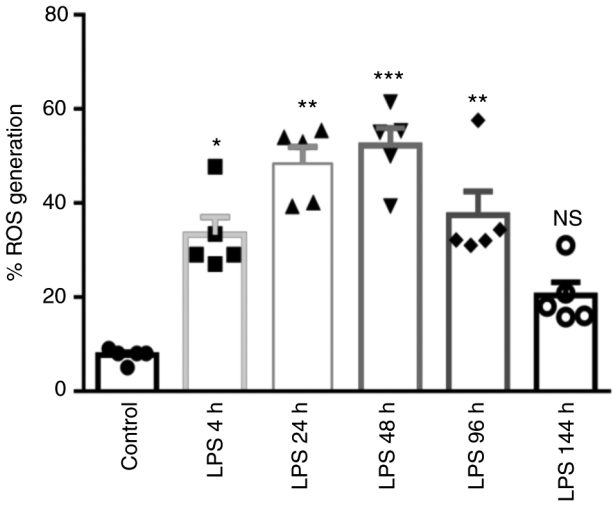

Figure 5. Time-dependent effects of LPS on ROS production in lung tissue. C57BL/6 mice were exposed to with 4 mg/kg LPS via intratracheal installation for 4, 24, 48, 96 and 144 h, and 0.9% NaCl was administered to the control mice orally. Lung tissues were collected after 4, 24, 48, 96 and 144 h of LPS exposure and from the control mice. ROS production was determined in lung tissue at different time points in the LPS groups and control group. Data are presented as the mean ± SEM (n=5 animals in each group). One-way ANOVA followed by the Bonferroni test were used to analyze significant differences among the different time points of the LPS group vs. the control. *P<0.05, **P<0.01 and ***P<0.001, vs. control. NS, not significant; LPS, lipopolysaccharide; ROS, reactive oxygen species.

lung tissue; however, the actual time point and mechanisms involved remain unclear. AMs have previously been reported to be involved in the accumulation of neutrophils in lung injury (37). In the present study, as shown by flow cytometry, the percentage of AMs (stained with F4/80^{+}CD11b^{-}) decreased from 4 to 144 h following exposure to LPS (Fig. 3C and F); however, the number of neutrophils (stained with LY6G PE-CY7A) significantly increased during this time period (LPS-4 h, LPS-24 h and LPS-48 h) compared to the control group (Fig. 3A and D).

Time-dependent effects of LPS on pro-inflammatory cytokines BALF and serum. Accumulating evidence suggests that macrophages and neutrophils are generally considered to be the major sources of IL-1β, CXCL1/KC, MIP-2, TNF-α (38-40). In the present study, to evaluate the time-dependent effects of LPS on the secretion of pro-inflammatory cytokines in BALF and serum, samples were collected at different time points from the mice in the LPS groups (4, 24, 48, 96, 144 h) and the control group. As shown in Fig. 4, the secretion of IL-1β, CXCL1/KC, MIP-2 and TNF-α in BALF and serum increased, and the maximal peak of cytokine secretion following LPS exposure was reached at 4 h; the levels then exhibited a decreasing trend in the from 96 to 144 h following the LPS instillation. These results demonstrated that LPS induced time-dependent changes in the secretion of the pro-inflammatory mediators, IL-1β, CXCL1/KC, MIP-2 and TNF-α, in the lungs and serum of C57BL/6 mice. Of note, in the control group, the cytokines were not constitutively expressed. Similar to the present study, Bosnar *et al* (41) found that the levels of CXCL1, TNF-α and IL-1β increased from 4 h following LPS stimulation in inflammatory cells and lung tissue.

Time-dependent effects of LPS on ROS production in lung tissue. The present study then examined the redox balance as an indicator of oxidative stress at different time points in LPS-induced lung tissue using an H_2DCFDA fluorescence probe. As shown in Fig. 5, the level of fluorescence intensity in the lung tissue significantly increased following LPS exposure at 4 h (36.39%), 24 h (48.33%), 48 h (55.40%), 96 h (39.04%) and 144 h (20.56%), whereas the highest level was recorded in the LPS-48 h group, with a decreasing trend observed at 144 h. These data suggested that ROS play a crucial role in hindering normal structure in a time-dependent manner after LPS induction.

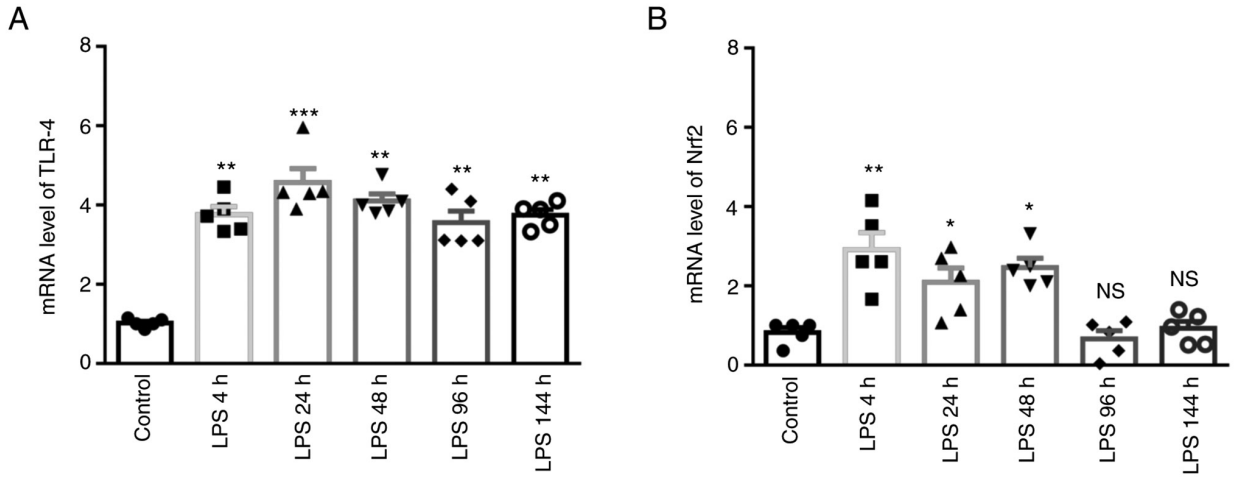

Figure 6. Time-dependent changes in the mRNA levels of TLR-4 and Nrf2 in lung tissue from mice with LPS-induced lung injury. C57BL/6 mice were exposed to with 4 mg/kg LPS via intratracheal installation for 4, 24, 48, 96 and 144 h, and 0.9% NaCl was administered to the control mice orally. Lung tissues were collected after 4, 24, 48, 96 and 144 h of LPS exposure and from the control mice. The mRNA levels of (A) TLR-4 and (B) Nrf2 were determined using reverse transcription-quantitative PCR. The results are expressed as the mean ± SEM (n=5 animals in each group). One-way ANOVA followed by the Bonferroni test were used to analyze significant differences among the different time points of the LPS group vs. the control. *P<0.05, **P<0.01 and ***P<0.001, vs. control. NS, not significant; LPS, lipopolysaccharide; TLR-4, Toll like receptor-4; Nrf2, nuclear factor E2-related factor 2.

Time-dependent changes in mRNA levels of TLR-4 and Nrf2 in lung tissue induced by LPS. As shown in Fig. 6A and B, the mRNA levels of TLR-4 significantly increased from 4 to 144 h following exposure to LPS compared with the control group, and the maximal mRNA expression levels were detected after 24 h (TLR-4) of LPS stimulation. The mRNA level of Nrf2 was significantly increased from 4 to 48 h following exposure to LPS. Notably, these data suggested that LPS affected the TLR-4 and Nrf2 mRNA levels in the early stages of lung injury.

Time-dependent responses of NLRP3 inflammasome activation in lung tissue. The present study then evaluated the effects of LPS on the activation of NLRP3 and cleaved caspase-1 in lung tissue in a time-dependent manner. The expression levels of NLRP3 and cleaved caspase-1 were markedly increased from 4 to 144 h following exposure to LPS; the densitometric analysis of the western blots revealed that the expression of NLRP3 at 24 h and that of cleaved caspase-1 at 48 h were higher when compared to those of the control group (Fig. 7). These data suggested that the NLRP3 inflammasome and cleaved caspase-1 activity were altered in a time-dependent manner following exposure to LPS.

Time-dependent responses of TLR-4, Keap-1, Nrf2 and HO-1 expression levels in lung tissue. Nrf2 serves as an important mediator regulating ROS-dependent inflammasome activation in ALI (27). In the present study, to investigate the possible mechanisms relevant to the Nrf2-related signaling pathway, the expression of the pNrf2, tNrf2, keap-1 and TLR-4 was first assayed using western blot analysis (Fig. 8A). LPS induced an increase in TLR-4 and Keap-1 expression in a time-dependent manner, with significant induction at 4, 24, 48 and 96 h (Fig. 8B and C). However, LPS induced the phosphorylation of Nrf2 according to Keap-1, suggesting that p-Nrf2 upregulation was independent of Keap-1 expression. As shown in Fig. 8D, the p-Nrf2 level was significantly increased in the LPS-4 h, LPS-24 h and LPS-48 h groups, respectively, compared with the t-Nrf2 level, as shown by densitometric analysis. In addition, HO-1 expression was significantly increased following LPS exposure from 4 to 96 h (Fig. 8E). Taken together, these results prompted us to further investigate the role of TLR-4 signaling components in regulating the initiation and expansion of Nrf2/HO-1 signaling in LPS-induced lung injury.

Time-dependent changes in the levels of cleaved caspase-8 and cleaved GSDMD in lung tissue. In pyroptosis, IL-1β secretion and caspase-1 activation are prominent characteristics. Caspase-8 has been reported to promote the cleavage of GSDMD and gasdermin E (GSDME) in murine macrophages, leading to pyroptotic cell death (28). In the present study, the levels of caspase-8, cleaved caspase-8, and the pyroptosis markers, GSDMD and cleaved GSDMD were measured at different time points (4, 24, 48, 96 and 144 h) following exposure to LPS (Fig. 9A). The protein expression levels of cleaved caspase-8 and cleaved GSDMD were higher at 48 and 4 h following exposure to LPS (Fig. 9B and C), while from 4 to 48 h following exposure to LPS, when compared to the control group, the levels of these proteins exhibited a significant difference. These results indicated that LPS plays a critical role in pyroptosis by upregulating the cleaved GSDMD levels in parallel with the activation of cleaved caspase-8 in ALI.

Discussion

The present study demonstrated the changing trends in macrophages and neutrophils along with subsets of T-cells in the lung tissues of mice with LPS-induced lung injury. Following the intratracheal administration of LPS, a significant increase in the activation of not only T-cells, but also macrophages and neutrophils was observed during the ALI process in a time-dependent manner. Furthermore, NLRP3/HO-1 activation, the subsequent release of pro-inflammatory cytokines and pyroptosis of lung tissue were found to be possible consequences of Nrf2/NLRP3 signaling.

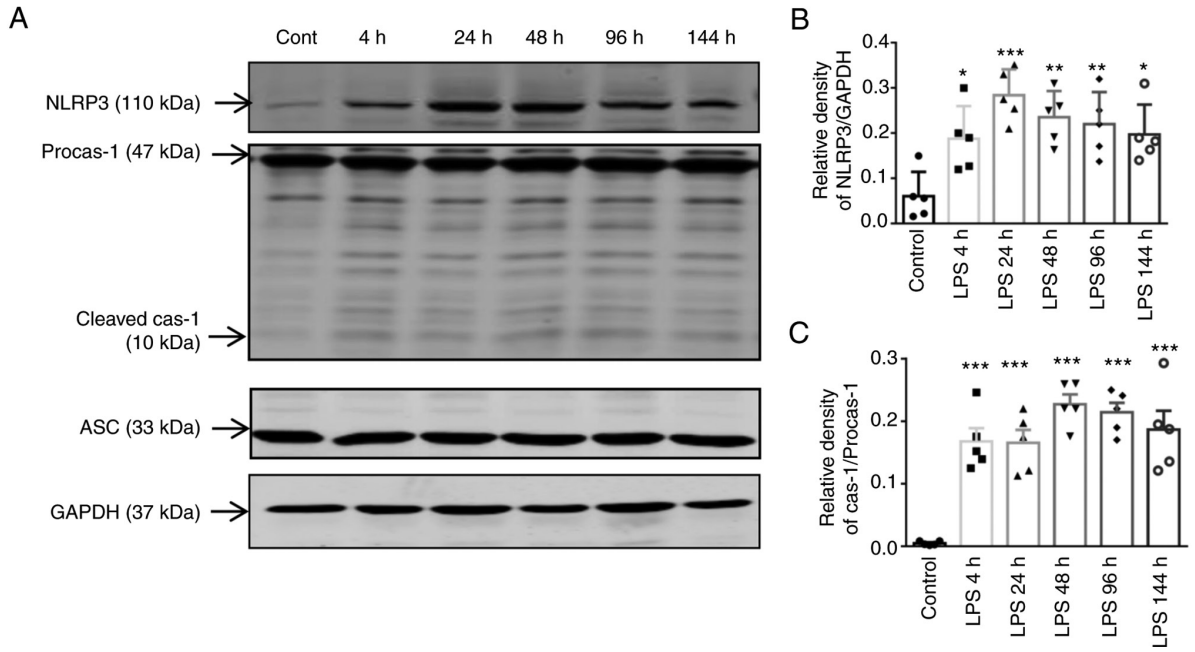

Figure 7. Time-dependent responses of NLRP3 inflammasome activation in lung tissue. C57BL/6 mice were exposed to with 4 mg/kg LPS via intratracheal installation for 4, 24, 48, 96 and 144 h, and 0.9% NaCl was administered to the control mice orally. Lung tissues were collected after 4, 24, 48, 96 and 144 h of LPS exposure and from the control mice. (A) Protein expression levels of NLRP3, ASC, procaspase-1/cleaved caspase-1 and GAPDH (internal control) were determined using western blot analysis with corresponding antibodies. (B and C) Relative expression levels of the proteins were determined using densitometric analysis. Data are presented as the mean ± SEM (n=5 animals in each group). One-way ANOVA followed by the Bonferroni test were used to analyze significant differences among the different time points of the LPS group vs. the control. *P<0.05, **P<0.01 and ***P<0.001, vs. control. NLRP3, nucleotide-binding oligomerization domain (NOD)-like receptor containing pyrin domain 3; LPS, lipopolysaccharide; ASC, apoptosis-associated speck-like protein containing a CARD; Procas-1, procaspase-1; cas-1, caspase-1.

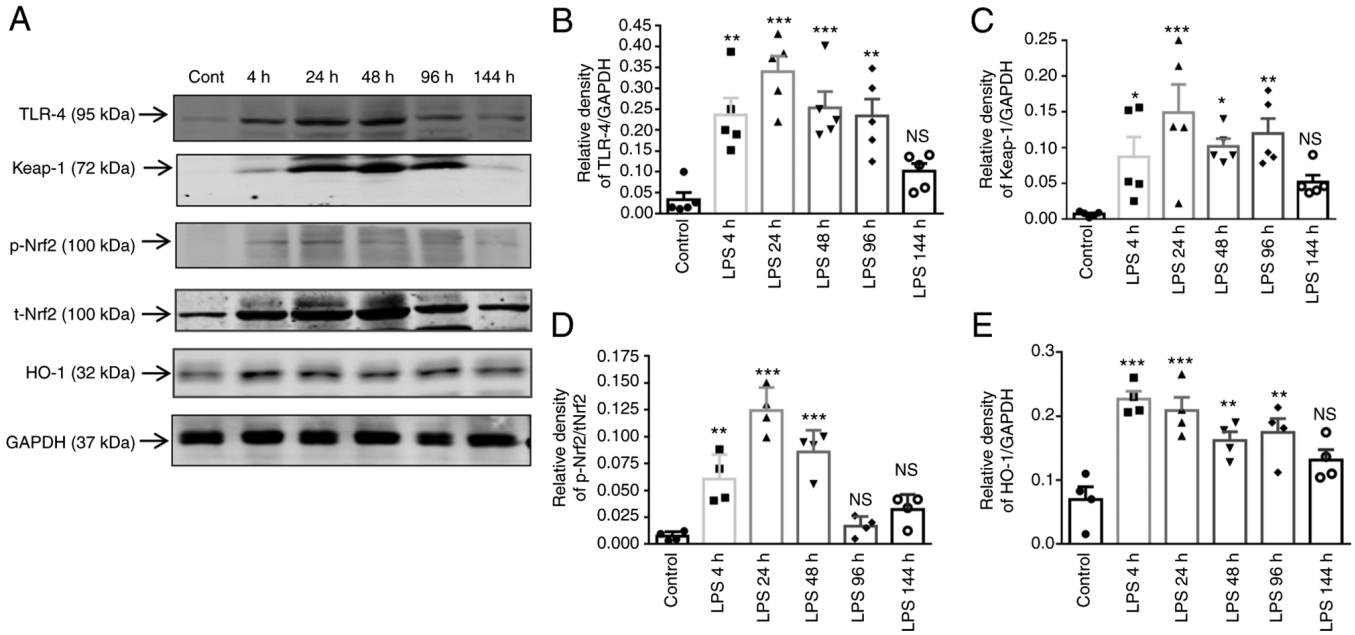

Figure 8. Time-dependent responses of TLR-4, Keap-1, Nrf2 and HO-1 expression in lung tissue. C57BL/6 mice were exposed to with 4 mg/kg LPS via intratracheal installation for 4, 24, 48, 96 and 144 h, and 0.9% NaCl was administered to the control mice orally. (A) Protein expression levels of TLR-4, Keap-1 and p-Nrf2, t-Nrf2, HO-1 and GAPDH (internal control) in the lungs of mice were assessed using western blot analysis; (B-E) Relative protein expression levels were determined using densitometric analysis. Data are presented as the mean ± SEM (n=4 animals in each group). One-way ANOVA followed by the Bonferroni test were used to analyze significant differences among the different time points of the LPS group vs. the control. *P<0.05, **P<0.01 and ***P<0.001, vs. control. *P<0.05, **P<0.01 and ***P<0.001, vs. control. NS, not significant; TLR-4, Toll like receptor-4; LPS, lipopolysaccharide; Nrf2, nuclear factor E2-related factor 2; p-, phosphorylated; t-, total.

LPS has been reported to induce neutrophil accumulation by stimulating macrophages in the infected area, which subsequently express distinct patterns of cytokines, chemokines and surface markers in ALI (42). The activation of

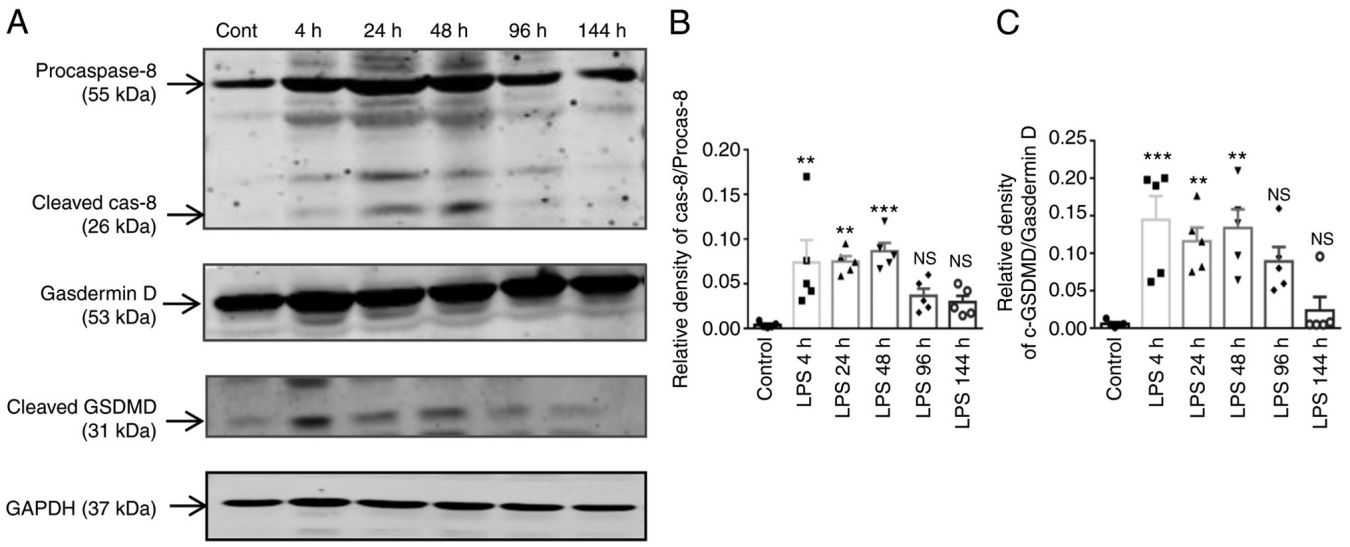

Figure 9. Time-dependent changes of cleaved caspase-8 and cleaved GSDMD in lung tissue. C57BL/6 mice were exposed to with 4 mg/kg LPS via intratracheal installation for 4, 24, 48, 96 and 144 h, and 0.9% NaCl was administered to the control mice orally. Lung tissues were collected, after 4, 24, 48, 96 and 144 h of LPS exposure and from the control mice. (A) The protein levels of procaspase-8, cleaved caspase-8, GSDMD and cleaved GSDMD in lung tissue were evaluated using western blot analysis; (B and C) the protein levels were quantified using densitometry. GAPDH was used as the loading control. The results are expressed as the mean ± SEM (n=5 animals in each group). One-way ANOVA followed by the Bonferroni test were used to analyze significant differences among the different time points of the LPS group vs. the control. **P<0.01 and ***P<0.001, vs. control. NS, not significant; GSDMD, gasdermin D; LPS, lipopolysaccharide.

macrophages and their subtypes (AMs and IMs) are dynamic processes that release pro-inflammatory cytokines during inflammation (12,43). Therefore, the present study analyzed neutrophils, macrophages and their types (AMs and IMs) in a mouse model of LPS-induced lung injury. It was found that LPS led to the recruitment of macrophages during the sub-chronic phase of lung injury. The suppression of AMs from LPS- 4 to 144 h was also demonstrated, which had a positive effect on lung injury and the increase in IMs. In the model of ALI, the number of neutrophils accumulated from 4 to 144 h of LPS treatment and was accompanied by the production of inflammatory mediators. Due to certain limitations, the present study we did not separate M1 and M2 macrophages. However, it was reported that the M2 phenotype was the main form of these resident AMs. In the acute phase of ALI/ARDS, resident alveolar macrophages, typically expressing the alternatively activated phenotype (M2), shift into the classically activated phenotype (M1) and release various potent pro-inflammatory mediators (44).

The differentiation of $CD4^+$ and $CD8^+$ T-cells has gained considerable attention in assessing the immune system (45). On the other hand, previous studies have suggested that LPS-induced TNF-α secretion in macrophages is mitigated when $CD4^+$ T-cells are depleted (46,47). Previously, challenge with LPS has been shown to increase the number of $CD4^+$ T-lymphocytes in the inflammatory infiltration during ALI (48,49). Furthermore, $CD4^+$ T-cells have been reported to be involved in the phenotypic transformation of macrophages and neutrophils (36). At the onset of injury, the activation of $CD8^+$ T-cells protects the injured area by laying the foundation for fibroblasts to enter and deposit the collagen scar, as well as to begin to resolve neutrophil-mediated inflammation (50,51). den Haan *et al* (52) suggested that the activation of TLRs led to the suppression of $CD8^+$ T-cell responses after priming with OVA plus LPS or poly(I:C). Therefore, the elucidation of the role of T-cells in promoting neutrophil and macrophage migration at different stages of ALI is of utmost urgency, as it may aid in diminishing inflammation in ALI. Herein, the data illustrated that the numbers of neutrophils and macrophage were increased along with the suppression of $CD8^+$ T-cells following exposure to LPS. However, LPS had no significant effect on $CD4^+$ T-cell activation. In addition, the present study evaluated the ratio of $CD4^+$:$CD8^+$ cells; the flow cytometry data revealed that the LPS installation markedly increased the percentage of $CD4^+$/$CD8^+$ cells in lung tissues. Similarly, the $CD4^+$/$CD8^+$ T-cell ratio has been found to be significantly elevated in virus-induced lower respiratory tract infection (17). Similar to the present study, Hussein *et al* (53) suggested that the higher CD4/CD8 ratio may be the result of recruited $CD4^+$ cells with decreased $CD8^+$ T-cell numbers, and/or the effects of the disease with the release of cytokines such as IL-1β, IL-6, TNF-α. The regulation of Th1, Th2, Th17 and Tregs, plays a critical role in immune mechanisms by interacting with other cells, and is associated with several inflammatory immune-mediated disorders, mainly sub-chronic and chronic inflammatory disorders (54). Moreover, the stimulation of these cells can trigger TGF-β, IL-6, IL-1β and MIP-2 and may also activate their transcriptional factor transcription factors, T-bet, GATA-3, RORγt and Forkhead box protein P3) (55,56). A previous study demonstrated that the stimulation of TNF-α triggered the expression of neutrophil-attracting chemokines, such as CXCL1 and CXCL2 (57). The present study investigated the mechanisms of regulatory T-cells and the secretion of the pro-inflammatory cytokines, TNF-α, CXCL1/KC, IL-1β and MIP-2. However, the results indicated that all pro-inflammatory cytokines aggravated lung inflammation from 4 h (acute phase) to 96 h (subacute phase) following the LPS administration. Moreover, compared with the control group, the protein expression and mRNA levels of TLR-4 were notably increased. Overall, a sustained LPS exposure

may exhaust the immune regulation between T-cell subsets, as well as the recruitment of macrophages, neutrophils and the secretion of pro-inflammatory cytokines through downstream TLR-4 signaling in the area of inflammation. Taken together, these data may aid in the future investigations of therapeutic approaches for immune abnormalities in models of LPS-induced lung injury.

There is increasing evidence to suggest that inflammasome complexes are activated by various danger signals, both endogenous and exogenous. Oxidative stress is known to play a critical role in ROS production and inflammasome activation (58). Even though researchers have suggested two different pathways through which NLRP3 senses changes in ROS, this remains an undefined issue. Thioredoxin-interacting protein binds to thioredoxin under homeostatic conditions, is liberated by ROS and can then interact with NLRP3, resulting in inflammasome inactivation (59,60). Another important pathway is NADPH oxidase and mitochondria dysfunction, and their aberrant actions subsequently activate the inflammasome (61). Of note, Nrf2 is a pivotal transcription factor that regulates intracellular redox balance by activating antioxidant genes (62). Therefore, it was primarily hypothesized that Nrf2 deletion promotes inflammasome formation by regulating a large battery of genes, such as HO-1, that reduces intracellular redox homeostasis. However, there is also an urgency to develop novel strategies with which to reduce inflammation in the early and late stages. The present study demonstrated that the intratracheal administration of LPS in mice led to the upregulation of Nrf2 activation (4 to 48 h) possibly involved in NLRP3 and caspase-1 expression through the aggravation of ROS levels from 4 to 96 h; IL-1β production and the recruitment of neutrophils and other cytokines and chemokines were also observed in the model of lung injury. Therefore, it is suggested that the positive feedback of the NLRP3/Nrf2/HO-1 pathway may be related to LPS-induced injury in lung tissue in the early stages of lung injury via the activation of immune cells and the release of various cytokines and chemokines. It has been suggested that bone marrow-derived macrophages (BMDMs) release mature IL-1β via Nrf2 signaling within 2 to 8 h following the activation of the NLRP3/caspase-1 complex; Nrf2 activation has also been reported to contribute to the LPS- and nigericin-induced ASC speck formation in BMDMs (27). It is therefore conceivable that Nrf2-signaling can promote IL-1β responses by sensing the loss of organelle integrity, similar to that shown by the NLRP3 inflammasome (61,63). Moreover, previous studies have indicated that HO-1 overexpression can lead to deleterious effects (64,65). However, the potential implications of the Nrf2/HO-1 pathway in the crosstalk regulation of imbalanced immune responses remain to be elucidated.

In addition to induction via death receptor ligation, caspase-8-mediated pyroptosis may also be involved in inflammasome components (66). Furthermore, the presence of caspase-1 and -11 inflammasomes may be involved in pyroptosis in macrophages (67), while the absence of cleaved caspase-1 promotes apoptosis (68). However, macrophages and neutrophils are considered as important participators in this process (69). In addition, neutrophil extracellular traps may contribute to ALI by promoting the pyroptosis of alveolar macrophages and systemic inflammation (70). Recently, a study indicated that the TLR4-mediated activation of caspase-8 led to the cleavage of GSDMD and the release IL-1β, resulting in pyroptosis (71). It has also been reported that caspase-1 cleaves GSDMD, and its N-terminal fragment translocates to the outer membrane, where macropores are formed, resulting in a lytic form of cell death (pyroptosis) (72,73). However, this process remains unclear in the model of LPS-induced ALI. Herein, it was found that the LPS-triggered caspase-8 and cleaved GSDMD activations were markedly enhanced in the presence of caspase-1 expression at similar time points from 4 to 48 h. This suggested that the time-dependent recruitment of caspase-8 is sensitive to the pyroptotic cascade, such as cleaved GSDMD expression in the model of ALI.

In conclusion, the present study demonstrated that acute and sub-chronic intratracheal administration of LPS enhanced multiple inflammatory responses, macrophages, AMs, IMs and neutrophils, as well as T-cell subsets from 4 to 96 h. The results of the present study suggest that the aberrant function of $CD4^+$/$CD8^+$ T-cell can exert profound effects on neutrophils and macrophage activation, and is associated with intervention in lung injury by modulating pro-inflammatory cytokines in both acute and sub-chronic stages. Moreover, the disruption of the redox balance and Nrf2/NLRP3 signaling pathway may also be involved in LPS-induced immune responses by activating pyroptosis. Therefore, the epigenetic program of T-cells and their functions, and the inhibition of Nrf2/NLRP3 target activation may lead to the development of novel therapeutic strategies for acute and sub-chronic lung disease.

Acknowledgements

The authors are grateful to the Core Facilities of Zhejiang University School of Medicine (Hangzhou, China), for technical assistance with flow cytometry and for processing analysis.

Funding

The present study was supported by the Zhejiang Provincial Natural Science Foundation (grant nos. LBY21H0100001, LYY18H310007 and LY18H310002), the Science Technology Department of Zhejiang Province Project (grant no. 2017C37132), the Medical Health Science and Technology Project of Zhejiang Provincial Health Commission (grant nos. 2018246654 and 2022KY928), and the Pre-research project of the National Natural Science Foundation of (grant no. 2018ZG12).

Availability of data and materials

The datasets used and/or analyzed during the current study are available from the corresponding author on reasonable request.

Authors' contributions

RD, NL and LZ participated in the western blot analysis, RT-qPCR, ELISA, histopathological analysis, ROS analysis and flow cytometry experiments. RD interpreted the results and wrote the manuscript. LN and LZ interpreted the key flow cytometry data. NL, YL and MNR contributed to the preparation of the animal model, and to the collection of the animal tissue specimens and interpreted the data. XC, ZH, XW, XZ

contributed to the harvesting of the animal tissues. XX and HT conceived all the experiments and revised the manuscript RD, NL and LZ confirm the authenticity of all the raw data. All authors confirmed and commented on previous versions of the manuscript along with have read and approved the final manuscript.

Ethics approval and consent to participate

The present study was approved by the Ethics Committee of the Zhejiang University (Hangzhou, China), and the experiments were performed in accordance with the National Institutes of Health Guidelines for the Use of Laboratory Animals.

Patient consent for publication

Not applicable.

Competing interests

The authors declare they have no competing interests.

References

1. Ranieri VM, Rubenfeld GD, Thompson BT, Ferguson ND, Caldwell E, Fan E, Camporota L and Slutsky AS: Acute respiratory distress syndrome: The Berlin definition. JAMA 307: 2526-2533, 2012.
2. Kushimoto S, Endo T, Yamanouchi S, Sakamoto T, Ishikura H, Kitazawa Y, Taira Y, Okuchi K, Tagami T, Watanabe A, *et al*: Relationship between extravascular lung water and severity categories of acute respiratory distress syndrome by the Berlin definition. Crit Care 17: R132, 2013.
3. Abdulnour REE and Levy BD: Acute lung injury and the acute respiratory distress syndrome. Med Manag Surg Patient A Textb Perioper Med Fifth Ed: 154-171, 2010.
4. Johnston LK, Rims CR, Gill SE, McGuire JK and Manicone AM: Pulmonary macrophage subpopulations in the induction and resolution of acute lung injury. Am J Respir Cell Mol Biol 47: 417-426, 2012.
5. Zhang A, Pan W, Lv J and Wu H: Protective effect of amygdalin on LPS-induced acute lung injury by inhibiting NF-κB and NLRP3 signaling pathways. Inflammation 40: 745-751, 2017.
6. Tianzhu Z and Shumin W: Esculin inhibits the inflammation of LPS-induced acute lung injury in mice via regulation of TLR/NF-κB pathways. Inflammation 38: 1529-1536, 2015.
7. Park EJ, Kim YM, Kim HJ and Chang KC: Luteolin activates ERK1/2- and Ca2+-dependent HO-1 induction that reduces LPS-induced HMGB1, iNOS/NO, and COX-2 expression in RAW264.7 cells and mitigates acute lung injury of endotoxin mice. Inflamm Res 67: 445-453, 2018.
8. Marsland BJ, Nembrini C, Grün K, Reissmann R, Kurrer M, Leipner C and Kopf M: TLR ligands act directly upon T cells to restore proliferation in the absence of protein kinase C-theta signaling and promote autoimmune myocarditis. J Immunol 178: 3466-3473, 2007.
9. Mandraju R, Murray S, Forman J and Pasare C: Differential ability of surface and endosomal TLRs to induce CD8 T cell responses in vivo. J Immunol 192: 4303-4315, 2014.
10. Imam F, Al-Harbi NO, Al-Harbi MM, Ansari MA, Zoheir KMA, Iqbal M, Anwer MK, Hoshani ARA, Attia SM and Ahmad SF: Diosmin downregulates the expression of T cell receptors, pro-inflammatory cytokines and NF-κB activation against LPS-induced acute lung injury in mice. Pharmacol Res 102: 1-11, 2015.
11. Boorsma CE, Draijer C and Melgert BN: Macrophage heterogeneity in respiratory diseases. Mediators Inflamm 2013: 769214, 2013.
12. Byrne AJ, Mathie SA, Gregory LG and Lloyd CM: Pulmonary macrophages: Key players in the innate defence of the airways. Thorax 70: 1189-1196, 2015.
13. Lee JW, Chun W, Lee HJ, Min JH, Kim SM, Seo JY, Ahn KS and Oh SR: The role of macrophages in the development of acute and chronic inflammatory lung diseases. Cells 10: 897, 2021.
14. Nakajima T, Suarez CJ, Lin KW, Jen KY, Schnitzer JE, Makani SS, Parker N, Perkins DL and Finn PW: T cell pathways involving CTLA4 contribute to a model of acute lung injury. J Immunol 184: 5835-5841, 2010.
15. Eberl G: RORγt, a multitask nuclear receptor at mucosal surfaces. Mucosal Immunol 10: 27-34, 2017.
16. Noack M and Miossec P: Th17 and regulatory T cell balance in autoimmune and inflammatory diseases. Autoimmun Rev 13: 668-677, 2014.
17. Connors TJ, Ravindranath TM, Bickham KL, Bickham KL, Gordon CL, Zhang F, Levin B, Baird JS and Farber DL: Airway CD8+ T cells are associated with lung injury during infant viral respiratory tract infection. Am J Respir Cell Mol Biol 54: 822-830, 2016.
18. Wong JJM, Leong JY, Lee JH, Albani S and Yeo JG: Insights into the immuno-pathogenesis of acute respiratory distress syndrome. Ann Transl Med 7: 504, 2019.
19. Kumar V: Toll-like receptors in sepsis-associated cytokine storm and their endogenous negative regulators as future immunomodulatory targets. Int Immunopharmacol 89: 107087, 2020.
20. Soy M, Keser G, Atagündüz P, Tabak F, Atagündüz I and Kayhan S: Cytokine storm in COVID-19: Pathogenesis and overview of anti-inflammatory agents used in treatment. Clin Rheumatol 39: 2085-2094, 2020.
21. Hennig P, Garstkiewicz M, Grossi S, Filippo MD, French LE and Beer HD: The crosstalk between Nrf2 and Inflammasomes. Int J Mol Sci 19: 562, 2018.
22. Garstkiewicz M, Strittmatter GE, Grossi S, Sand J, Fenini G, Werner S, French LE and Beer HD: Opposing effects of Nrf2 and Nrf2-activating compounds on the NLRP3 inflammasome independent of Nrf2-mediated gene expression. Eur J Immunol 47: 806-817, 2017.
23. Maier NK, Leppla SH and Moayeri M: The cyclopentenone prostaglandin 15d-PGJ 2 inhibits the NLRP1 and NLRP3 inflammasomes. J Immunol 194: 2776-2785, 2015.
24. Tonelli C, Chio IIC and Tuveson DA: Transcriptional regulation by Nrf2. Antioxid Redox Signal 29: 1727-1745, 2018.
25. Kelley N, Jeltema D, Duan Y and He Y: The NLRP3 inflammasome: An overview of mechanisms of activation and regulation. Int J Mol Sci 20: 3328, 2019.
26. Possomato-Vieira, José S and Khalil RAK: Mechanism and regulation of NLRP3 inflammasome activation. Physiol Behav 176: 139-148, 2016.
27. Zhao C, Gillette DD, Li X, Zhang Z and Wen H: Nuclear factor E2-related factor-2 (Nrf2) is required for NLRP3 and AIM2 inflammasome activation. J Biol Chem 289: 17020-17029, 2014.
28. Sarhan J, Liu BC, Muendlein HI, Li P, Nilson R, Tang AY, Rongvaux A, Bunnell SC, Shao F, Green DR and Poltorak A: Caspase-8 induces cleavage of gasdermin D to elicit pyroptosis during Yersinia infection. Proc Natl Acad Sci USA 115: E10888-E10897, 2018.
29. Muendlein HI, Jetton D, Connolly WM, Eidell KP, Magri Z, Smirnova I and Poltorak A: CFLIPL protects macrophages from LPS-induced pyroptosis via inhibition of complex II formation. Science 367: 1379-1384, 2020.
30. Xia S, Hollingsworth LR and Wu H: Mechanism and regulation of gasdermin-mediated cell death. Cold Spring Harb Perspect Biol 12: 1-14, 2020.
31. Cen M, Ouyang W, Zhang W, Yang L, Lin X, Dai M, Hu H, Tang H, Liu H, Xia J and Xu F: MitoQ protects against hyperpermeability of endothelium barrier in acute lung injury via a Nrf2-dependent mechanism. Redox Biol 41: 101936, 2021.
32. Tseng TL, Chen MF, Tsai MJ, Hsu YH, Chen CP and Lee TJF: Oroxylin-a rescues LPS-induced acute lung injury via regulation of NF-κB signaling pathway in rodents. PLoS One 7: e47403, 2012.
33. Matute-Bello G, Downey G, Moore BB, Groshong SD, Matthay MA, Slutsky AS and Kuebler WM: An official american thoracic society workshop report: Features and measurements of experimental acute lung injury in animals. Am J Respir Cell Mol Biol 44: 725-738, 2011.
34. Livak KJ and Schmittgen TD: Analysis of relative gene expression data using real-time quantitative PCR and the 2(-Delta Delta C(T)) method. Methods 25: 402-408, 2001.
35. Socci DJ, Bjugstad KB, Jones HC, Pattisapu JV and Arendash GW: Evidence that oxidative stress is associated with the pathophysiology of inherited hydrocephalus in the H-Tx rat model. Exp Neurol 155: 109-117, 1999.

36. Roberts CA, Dickinson AK and Taams LS: The interplay between monocytes/macrophages and CD4+ T cell subsets in rheumatoid arthritis. Front Immunol 6: 571, 2015.
37. Dagvadorj J, Shimada K, Chen S, Jones HD, Tumurkhuu G, Zhang W, Wawrowsky KA, Crother TR and Arditi M: Lipopolysaccharide induces alveolar macrophage necrosis via CD14 and the P2x7 receptor leading to Interleukin-1α release. Immunity 42: 640-653, 2016.
38. Altemeier WA, Zhu X, Berrington WR, Harlan JM and Liles WC: Fas (CD95) induces macrophage proinflammatory chemokine production via a MyD88-dependent, caspase-independent pathway. J Leukoc Biol 82: 721-728, 2007.
39. Hatanaka E, Monteagudo PT, Marrocos MSM and Campa A: Neutrophils and monocytes as potentially important sources of proinflammatory cytokines in diabetes. Clin Exp Immunol 146: 443-447, 2006.
40. An SJ, Pae HO, Oh GS, Choi BM, Jeong S, Jang SI, Oh H, Kwon TO, Song CE and Chung HT: Inhibition of TNF-α, IL-1β, and IL-6 productions and NF-κB activation in lipopolysaccharide-activated RAW 264.7 macrophages by catalposide, an iridoid glycoside isolated from Catalpa ovata G. Don (Bignoniaceae). Int Immunopharmacol 2: 1173-1181, 2002.
41. Bosnar M, Bošnjak B, Čužić S, Hrvacic B, Marjanovic N, Glojnaric I, Culic O, Parnham MJ and Haber VE: Azithromycin and clarithromycin inhibit lipopolysaccharide-induced murine pulmonary neutrophilia mainly through effects on macrophage-derived granulocyte-macrophage colony-stimulating factor and interleukin-1β. J Pharmacol Exp Ther 331: 104-113, 2009.
42. Risso K, Kumar G, Ticchioni M, Sanfiorenzo C, Dellamonica J, Guillouet-de Salvador F, Bernardin G, Marquette CH and Roger PM: Early infectious acute respiratory distress syndrome is characterized by activation and proliferation of alveolar T-cells. Eur J Clin Microbiol Infect Dis 34: 1111-1118, 2015.
43. Janssen WJ, Barthel L, Muldrow A, Oberley-Deegan RE, Kearns MT, Jakubzick C and Henson PM: Fas determines differential fates of resident and recruited macrophages during resolution of acute lung injury. Am J Respir Crit Care Med 184: 547-560, 2011.
44. Chen X, Tang J, Shuai W, Meng J, Feng J and Han Z: Macrophage polarization and its role in the pathogenesis of acute lung injury/acute respiratory distress syndrome. Inflamm Res 69: 883-895, 2020.
45. Williams MA, Rangasamy T, Bauer SM, Killedar S, Karp M, Kensler TW, Yamamoto M, Breysse P, Biswal S and Georas SN: Disruption of the transcription factor Nrf2 promotes pro-oxidative dendritic cells that stimulate Th2-like immunoresponsiveness upon activation by ambient particulate matter. J Immunol 181: 4545-4559, 2008.
46. D'Souza NB, Mandujano FJ, Nelson S, Summer WR and Shellito JE: CD4+ T lymphocyte depletion attenuates lipopolysaccharide-induced tumor necrosis factor secretion by alveolar macrophages in the mouse. Lymphokine Cytokine Res 13: 359-366, 1994.
47. Crowe CR, Chen K, Pociask DA, Alcorn JF, Krivich C, Enelow RI, Ross TM, Witztum JL and Kolls JK: Critical role of IL-17RA in immunopathology of influenza infection. J Immunol 183: 5301-5310, 2009.
48. Chai YS, Chen YQ, Lin SH, Xie K, Wang CJ, Yang YZ and Xu F: Curcumin regulates the differentiation of naïve CD4+T cells and activates IL-10 immune modulation against acute lung injury in mice. Biomed Pharmacother 125: 109946, 2020.
49. Philippakis GE, Lazaris AC, Papathomas TG, Zissis C, Agrogiannis G, Thomopoulou G, Nonni A, Xiromeritis K, Nikolopoulou-Stamati P, Bramis J, *et al*: Adrenaline attenuates the acute lung injury after intratracheal lipopolysaccharide instillation: An experimental study. Inhal Toxicol 20: 445-453, 2008.
50. Haring JS, Badovinac VP and Harty JT: Inflaming the CD8+ T cell response. Immunity 25: 19-29, 2006.
51. Ilatovskaya DV, Pitts C, Clayton J, Domondon M, Troncoso M, Pippin S and DeLeon-Pennell KY: CD8+ T-cells negatively regulate inflammation post-myocardial infarction. Am J Physiol Hear Circ Physiol 317: H581-H596, 2019.
52. den Haan JMM, Kraal G and Bevan MJ: Cutting edge: Lipopolysaccharide induces IL-10-producing regulatory CD4 + T cells that suppress the CD8 + T cell response. J Immunol 178: 5429-5433, 2007.
53. Hussein MR, Hassan HI, Hofny ERM, Elkholy M, Fatehy NA, Elmoniem AEA, El-Din AME, Afifi OA and Rashed HG: Alterations of mononuclear inflammatory cells, CD4/CD8+ T cells, interleukin 1β, and tumour necrosis factor α in the bronchoalveolar lavage fluid, peripheral blood, and skin of patients with systemic sclerosis. J Clin Pathol 58: 178-184, 2005.
54. Cabrera-Perez J, Condotta SA, Badovinac VP and Griffith TS: Impact of sepsis on CD4 T cell immunity. J Leukoc Biol 96: 767-777, 2014.
55. Hori S, Nomura T and Sakaguchi S: Control of regulatory T cell development by the transcription factor Foxp3. J Immunol 198: 981-985, 2017.
56. Ivanov II, McKenzie BS, Zhou L, Tadokoro CE, Lepelley A, Lafaille JJ, Cua DJ and Littman DR: The orphan nuclear receptor RORγt directs the differentiation program of proinflammatory IL-17+ T helper cells. Cell 126: 1121-1133, 2006.
57. Griffin GK, Newton G, Tarrio ML, Bu DX, Maganto-Garcia E, Azcutia V, Alcaide P, Grabie N, Luscinskas FW, Croce KJ and Lichtman AH: IL-17 and TNFα sustain neutrophil recruitment during inflammation through synergistic effects on endothelial activation1. J Immunol 188: 6287-6299, 2012.
58. Wen H, Miao EA and Ting JPY: Mechanisms of NOD-like receptor-associated inflammasome activation. Immunity 39: 432-441, 2013.
59. Abais JM, Xia M, Zhang Y, Boini KM and Li PL: Redox regulation of NLRP3 inflammasomes: ROS as trigger or effector? Antioxidants Redox Signal 22: 1111-1129, 2015.
60. Zhou R, Tardivel A, Thorens B, Choi I and Tschopp J: Thioredoxin-interacting protein links oxidative stress to inflammasome activation. Nat Immunol 11: 136-140, 2010.
61. Zhou R, Yazdi AS, Menu P and Tschopp J: A role for mitochondria in NLRP3 inflammasome activation. Nature 469: 221-226, 2011.
62. Vomund S, Schäfer A, Parnham MJ, Brüne B and Von Knethen A: Nrf2, the master regulator of anti-oxidative responses. Int J Mol Sci 18: 2772, 2017.
63. Hornung V, Bauernfeind F, Halle A, Samstad EO, Kono H, Rock KL, Fitzgerald KA and Latz E: Silica crystals and aluminum salts activate the NALP3 inflammasome through phagosomal destabilization. Nat Immunol 9: 847-856, 2008.
64. Jais A, Einwallner E, Sharif O, Gossens K, Lu TTH, Soyal SM, Medgyesi D, Neureiter D, Paier-Pourani J, Dalgaard K, *et al*: Heme oxygenase-1 drives metaflammation and insulin resistance in mouse and man. Cell 158: 25-40, 2014.
65. Tronel C, Rochefort GY, Arlicot N, Bodard S, Chalon S and Antier D: Oxidative stress is related to the deleterious effects of heme oxygenase-1 in an in vivo neuroinflammatory rat model. Oxid Med Cell Longev 2013: 264935, 2013.
66. Raghawan AK, Sripada A, Gopinath G, Pushpanjali P, Kumar Y, Radha V and Swarup G: A disease-associated mutant of NLRC4 shows enhanced interaction with SUG1 leading to constitutive fadddependent caspase-8 activation and cell death. J Biol Chem 292: 1218-1230, 2017.
67. Pierini R, Juruj C, Perret M, Jones CL, Mangeot P, Weiss DS and Henry T: AIM2/ASC triggers caspase-8-dependent apoptosis in francisella-infected caspase-1-deficient macrophages. Cell Death Differ 19: 1709-1721, 2012.
68. Antonopoulos C, Russo HM, El Sanadi C, Martin BN, Li X, Kaiser WJ, Mocarski ES and Dubyak GR: Caspase-8 as an effector and regulator of NLRP3 inflammasome signaling. J Biol Chem 290: 20167-20184, 2015.
69. Robinson N, Ganesan R, Hegedűs C, Kovács K, Kufer TA and Virág L: Programmed necrotic cell death of macrophages: Focus on pyroptosis, necroptosis, and parthanatos. Redox Biol 26: 101239, 2019.
70. Haitao Lee PP: Neutrophil extracellular traps promoted alveolar macrophages pyroptosis in LPS induced ALI/ARDS. Eur Respir J 52: PA4284, 2018.
71. Orning P, Weng D, Starheim K, Ratner D, Best Z, Lee B, Brooks A, Xia S, Wu H, Kelliher MA, *et al*: Pathogen blockade of TAK1 triggers caspase-8-dependent cleavage of gasdermin D and cell death. Science 362: 1064-1069, 2018.
72. Shi J, Zhao Y, Wang K, Shi X, Wang Y, Huang H, Zhuang Y, Cai T, Wang F and Shao F: Cleavage of GSDMD by inflammatory caspases determines pyroptotic cell death. Nature 526: 660-665, 2015.
73. Kayagaki N, Stowe IB, Lee BL, O'Rourke K, Anderson K, Warming S, Cuellar T, Haley B, Roose-Girma M, Phung QT, *et al*: Caspase-11 cleaves gasdermin D for non-canonical inflammasome signalling. Nature 526: 666-671, 2015.